Tellus (2003), 55B, 244–257

TELLUS
ISSN 0280–6509

CO_2 and water vapor exchange of a larch forest in northern Japan

By TAKASHI HIRANO[1]*, RYUICHI HIRATA[1], YASUMI FUJINUMA[2], NOBUKO SAIGUSA[3], SUSUMU YAMAMOTO[3], YOSHINOBU HARAZONO[4], MASAYUKI TAKADA[2], KOH INUKAI[2] and GEN INOUE[2], [1]*Graduate School of Agriculture, Hokkaido University, Sapporo 060-8589, Japan;* [2]*Center for Global Environmental Research, National Institute for Environmental Studies, Tsukuba 305-8506, Japan;* [3]*National Institute of Advanced Industrial Science and Technology, Tsukuba 305-8604, Japan;* [4]*International Arctic Research Center, University of Alaska Fairbanks, AK 99775, USA*

(Manuscript received 9 January 2002; in final form 13 December 2002)

ABSTRACT

In the northern part of East Asia, forests dominated by larch are extensively distributed and probably play an important role in the global carbon cycle. However, a knowledge of the CO_2 balance of larch forests based on long-term flux measurements is very restricted in East Asia. Thus, a long-term flux measurement has been started in 2000 at a larch plantation on a flat terrain in Hokkaido, Japan to obtain more information on the CO_2 and energy balances of larch forests. From September 2000 to August 2001 the net ecosystem CO_2 exchange (NEE) changed seasonally in accordance with the annual cycles of phenology and climate. NEE was negative for six months of the growing season, May–September; the larch ecosystem was a carbon sink with a peak intensity of –0.38 mol m^{-2} d^{-1} for this period. In the leafless season from November to April the forest ecosystem was a carbon source with an intensity ranging between 0 and 0.05 mol m^{-2} d^{-1}. Annual NEE from September 2000 to August 2001 was −24.4 to −32.4 mol m^{-2} yr^{-1} (= −293 to −389 gC m^{-2} yr^{-1}); this value is compatible with those reported from other temperate forests. Annual evapotranspiration for the same period was 367 mm, which was only 29% of annual precipitation.

1. Introduction

The increase in atmospheric CO_2 concentration and consequent global warming are now the greatest environmental issue in the world. This CO_2 increase is attributed to the global-scale imbalance of CO_2 source and sink intensities. Although the CO_2 increase is chiefly explained by fossil-fuel combustion and deforestation, the global carbon balance is not yet closed. The anthropogenically released CO_2 must be absorbed by “missing sinks,” and the terrestrial biosphere is believed to be an important component of these (Houghton et al., 1998). For the closure of the carbon balance, it is necessary to evaluate the CO_2 exchange between the various types of terrestrial ecosystems and the atmosphere through long-term continuous measurements of CO_2 flux. In the 1990s the long-term monitoring of CO_2, water vapor and sensible heat fluxes over forest ecosystems was started using towers, and these tower sites were networked in Europe (EUROFLUX) and North America (AmeriFlux). In Asia a flux monitoring network was established in 2000 (AsiaFlux), and AsiaFlux is a regional subnetwork of the global network (FLUXNET) together with EUROFLUX and AmeriFlux (Baldocchi et al., 2001). Since Asia covers diverse terrestrial ecosystems from tropical rain forests in Indonesia to tundra in Siberia, AsiaFlux can help fill the gaps in our knowledge of the global CO_2 cycle and the climatic system.

*Corresponding author.
e-mail: hirano@env.agr.hokudai.ac.jp

Forests dominated by the deciduous conifer larch (*Larix gmelinii*) are extensively distributed in northern East Asia (Gower and Richards, 1990). In Central Japan Japanese larch (*Larix kaempferi*) is distributed as the southern edge of the larch distribution in East Asia. Since it is tolerant to cold and grows rapidly, Japanese larch is one of the most important plantation species in northern Japan. The larch plantation covers about 4700 km^2 of Hokkaido Island, the northernmost island of Japan, and nowadays it is a principal forest ecosystem in northern Japan. Recent studies suggest that the boreal forest in the Northern Hemisphere is a large CO_2 sink (Denning et al., 1995; Otto-Bliesner and Upchurch, 1997). The extensive larch forests in East Asia probably play an important role in the global carbon cycle. However, knowledge of the CO_2 balance of larch forests based on long-term flux measurements is very restricted in East Asia (Machimura and Fukuda, 2001). Thus, a long-term flux measurement was started in 2000 by the National Institute for Environmental Studies (NIES) at a larch forest in Hokkaido, Japan to obtain more information on the CO_2 and energy balances (Fujinuma et al., 2001). The forest site was established as a key site of AsiaFlux. This paper describes the first year of flux measurements.

2. Materials and methods

2.1. Site description

The study site is a Japanese larch (*Larix kaempferi*) plantation in Tomakomai National Forest managed by the Hokkaido Regional Office of the Forestry Agency. The larch forest was planted in 1957–1959 and is located at 42°44′N, 141°31′E on flat terrain in Hokkaido, northern Japan. It is about 14 km from the Pacific Ocean and the elevation is about 140 m above sea level. The area of the larch forest is about 100 ha, and the forest is surrounded by a deciduous broadleaf forest and an evergreen conifer forest. In the larch forest some deciduous broadleaf trees, such as birch (*Betula ermanii* and *Betula platyphylla*) and Japanese elm (*Ulmus japonica*), invade into the gaps, and individual trees of spruce (*Picea jezonensis*) grow sparsely. Stand densities of trees with a stem diameter at breast height (DBH) larger than 5 cm were 673, 459, 18 and 1150 stems ha^{-1} for larch, broadleaf trees, spruce and all species, respectively, in 1999. DBH of larch ranged from 6 to 48 cm, and the median was 20–22 cm. Although all the larch trees were planted at about the same time, their growth is quite varied. In contrast, DBH of broadleaf trees was around 10 cm. Basal area densities at breast height of larch, broadleaf trees and spruce were 19.0, 4.1 and 0.4 m^2 ha^{-1}, respectively. Thus, the occupation of larch in the canopy was 81% on a stem area basis, while it was 59% on a stem number basis.

The canopy was homogeneous and its height was about 15 m. Leaf area index (LAI) of the canopy was 2.1 m^2 m^{-2} at the maximum (see Fig. 2 later). In the trunk space there were scattered stands of shrubs (*Hydrangea paniculata*, *Sorbus alnifolia*, *Tilia japonica* and *Acer palmatum*) and woody vines, such as *Rhus ambigua* and *Hydrangea petiolaris*, climbing the larch stems. The forest floor was densely covered with fern (*Dryopteris crassirhizoma*). Height and LAI of the fern were 0.5–0.8 m and about 3 m^2 m^{-2} in late June 2001, respectively. The soil was a volcanogenous regosol with high water permeability and poor nutrients. The thickness of the surface organic layer (A horizon) was about 10 cm.

2.2. Facilities

On the site there are two scaffold-type towers; one is 42 m tall for flux and micrometeorological measurements, the another is 25 m tall for ecophysiological studies. The distance between the two towers is about 600 m. The area used for ecophysiological studies is isolated from the flux tower to avoid artificial effects on flux measurements. The 42 m tower with a cross-section of 1.3 m (east–west) × 1.9 m (north–south) was set up in the center of the forest.

2.3. Micrometeorological measurements

Micrometeorology has been monitored since July 2000 on the tower, and 1.5 m tall tripods are set up on the forest floor within 30 m from the tower.

Solar radiation was measured at heights of 41, 18, 14 and 5 m, and at six points at 1.5 m with pyranometers (MS-601, Eko, Japan). Four components of radiation, including downward and upward short-wave and long-wave radiation, were measured at 40, 18 and 1.5 m with radiometers (MR40, Eko, Japan); net radiation (R_n) and albedo were calculated from these components. Photosynthetic photon flux density (PPFD) was measured at 40, 18 and 5 m, and at three points at 1.5 m with quantum sensors (LI-190S, Licor, USA). Downward and upward spectral radiation for six wavelength bands was measured at 42 m with spectral radiometers

(MS-131WP, Eko, Japan). The normalized difference vegetation index (NDVI) was calculated from an equation, using the daytime data between 09:00 and 15:00,

$$\mathrm{NDVI} = \frac{\mathrm{NIR} - \mathrm{R}}{\mathrm{NIR} + \mathrm{R}} \quad (1)$$

where R and NIR are upward radiation intensities for wavelength bands of 590–685 and 695–850 nm, respectively.

Wind speed and direction were measured at 42, 27, 22, 18, 14, 8, 5 and 1.5 m with sonic anemometers (MA-130, Eko, Japan and DA-600-3TV, Kaijo, Japan). Precipitation was measured at 41 m and at three points at 1.5 m with tipping-bucket rain gauges (52 202, R. M. Young, USA). Atmospheric pressure was measured at 41, 18, 8, 5 and 1.5 m with barometers (PTB101, Vaisala, Finland). Air temperature and relative humidity were measured at 41, 27, 22, 18, 14, 8, 5 and 1.5 m with platinum resistance thermometers and capacitive hygrometers (HMP45D, Vaisala, Finland); the probe is installed in a ventilated radiation shield. Moreover, soil temperature was measured at depths of 5, 10, 20 and 50 cm at three points near the tripods with platinum resistance thermometers. Soil water content was measured at 5 and 10 cm at three points with TDR sensors (CS615, CSI, USA). Soil heat flux (G) was measured at five points at 5 cm with heat flux plates (MF-81, Eko, Japan). Signals from the sensors were measured every second, and 10 and 30 min means were recorded using four dataloggers (CR23X, CSI, USA). The sensors were maintained weekly and an intensive calibration was made once a year.

2.4. *Measurement and calculation of fluxes*

CO_2, water vapor and heat fluxes have been continuously measured since September 2000 using the eddy covariance technique on the tower top at 42 m, about 27 m above the canopy surface. A three-dimensional sonic anemometer–thermometer (SAT) (DA-600-3TV, Kaijo, Japan) and an open-path infrared CO_2/H_2O analyzer (OP-2, Data design, USA), developed at NOAA/ATDD (Auble and Meyers, 1992) were installed in June 2000 to measure fluctuations in wind speed, virtual temperature, CO_2 density and water vapor density. In the middle of October 2000 another open-path CO_2/H_2O analyzer (LI7500, Licor, USA) was added. The flux sensors were aligned along the east–west direction on the south edge of the tower top, and the SAT was positioned between the two open-path analyzers to minimize flow distortion; the dominant wind direction was south. Sensor separation between the SAT and each open-path analyzer was 0.3 m. Fluctuations in CO_2 and water vapor densities were also measured by a closed-path CO_2/H_2O analyzer (LI6262, Licor, USA). The open-path sensors were dynamically calibrated with the closed-path sensor for CO_2 and a Vaisala hygrometer for water vapor. The closed-path sensor was automatically calibrated once a day with zero and span gases of CO_2. Moreover, the calibration of the open-path sensors was periodically made with standard CO_2 gases and a dew point generator (LI610, Licor, USA). All of the raw data were sampled at 10 Hz using an analog datalogger (DR-M3, TEAC, Japan) with a magneto-optical (MO) disk. In this paper we only describe the fluxes measured by the open-path system. Details of the closed-path system are in preparation.

Half-hourly mean fluxes of CO_2, water vapor and sensible heat were calculated from the recorded data according to the following procedure: (1) removal of electrical noise spikes, (2) three-dimensional coordinate rotation to make the mean lateral and vertical wind speeds zero (McMillen, 1988), (3) calculation of covariance using half-hourly block average, (4) water vapor correction for virtual temperature (Hignett, 1992), (5) crosswind speed correction for virtual temperature (Kaimal and Gaynor, 1991), and (6) density fluctuation (WPL) correction (Webb et al., 1980). The data were missing when calibration and maintenance were made. Under conditions of rain, snow and fog, the data set often included too much noise for the fluxes to be calculated. Consequently, gaps occurred in 25, 17 and 10% of the time series of half-hourly flux for CO_2, water vapor and sensible heat, respectively. These gaps were filled using a nonlinear regression for CO_2 flux (Falge et al., 2001a; see Figs. 7 and 8) and look-up table for water vapor and sensible heat fluxes (Falge et al., 2001b). The tables were made for three periods, which were leaf (May to October), leafless (November and 11–30 April) and snow (December to 10 April) seasons. In the tables the fluxes were classified by net radiation and vapor pressure deficit (VPD) at a height of 14 m. Since CO_2 concentration profiles have been unavailable until the middle of July 2001, the change in CO_2 storage in the layer below the flux-measuring level was simply calculated with the change in CO_2 concentration at 42 m (Greco and Baldocchi, 1996) measured by the closed-path analyzer (LI6262). Net ecosystem exchange of CO_2 (NEE) was then calculated as the sum of the CO_2 flux and CO_2 storage. The sign of NEE is negative when the CO_2

absorption of the ecosystem is larger than the CO_2 release.

Signals from the open-path sensor, OP-2, were noisier than those from LI7500, and large trend sometimes occurred in the OP-2′s signals in October and March. This trend was probably caused by the exposure of the sensor's windows to direct solar radiation. Half-hourly covariance of eddy fluctuations in vertical wind speed (w') and CO_2 density (c'), and water vapor density (q') are compared between OP-2 and LI7500 in late October 2000 and late May 2001 (Fig. 1). Although the covariance from the two sensors was not identical, there was a linear regression with large r^2. We decided that LI7500 was more accurate than OP-2, because a field experiment for the comparison of flux measuring systems between AmeriFlux and AsiaFlux that was held at our site in August 2001 showed that the CO_2 and water vapor fluxes measured by the 3D-SAT (DA-600-3TV, Kaijo) and LI7500 agreed well with those measured by the AmeriFlux reference set of instruments (Nakai et al., 2002). Thus, the LI7500 data were used for the flux calculations from the middle of October 2000 to May 2001, and in August 2001. When LI7500 was not installed, the eddy covariance from the OP-2 data was corrected using the regression equations shown in Fig. 1; the regression lines obtained in October and May were applied for September and the beginning of October 2000, and for June and July 2001, respectively.

The fetch was between 300 m for the north and 800 m for the west and east; it was about 400 m for the south, the dominant wind direction. An evergreen conifer forest and a deciduous broadleaf forest were adjacent to the larch forest on the south and north sides, respectively. Flux footprint calculations from an analytical model (Kormann and Mexiner, 2001) showed that 80% of the eddy flux measured at 42 m originated within 200–1000 m from the tower, with a peak at 50–100 m in the daytime; the footprint depends on the atmospheric stability. At night, 80% of the flux originated within 500–5000 m, with a peak at 50–300 m. This suggests that the fetch was insufficient or the measuring height was too high under stable conditions, which was common at night.

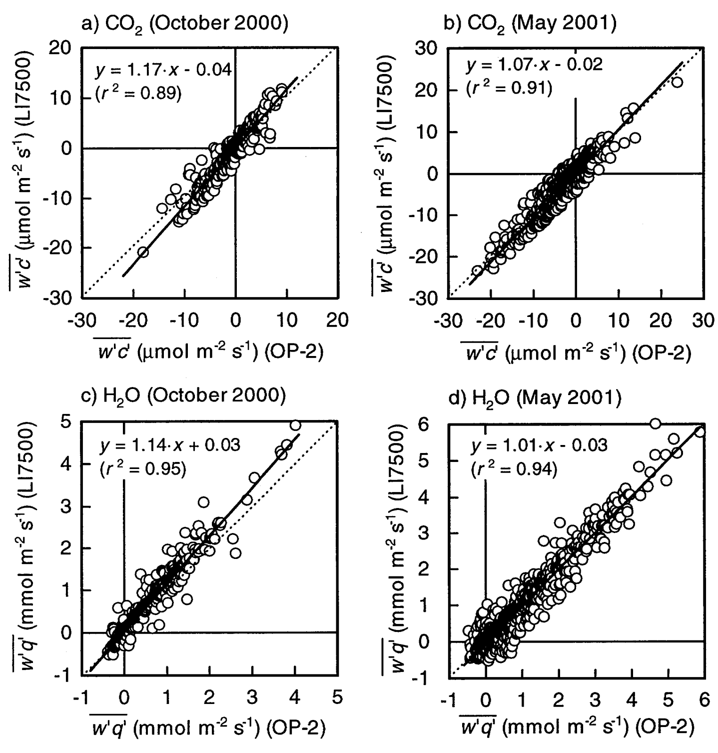

Fig. 1. Comparison of half-hourly covariance of eddy fluctuations in vertical wind speed (w') and CO_2 density (c'), and water vapor density (q') between OP-2 and LI7500 in late October 2000 and late May 2001.

Plant area index (PAI) was measured every 2–3 wk from April to November 2001 using a plant canopy analyzer (LAI2000, Licor, USA) at six points near the pyranometers installed at a height of 1.5 m around the flux tower. Leaf area index (LAI) was determined as the residual between PAI and wood area index (WAI) measured with the same method in the end of November, after defoliation; WAI was 1.4 m^2 m^{-2}. By applying Beer' law of radiation, an extinction coefficient was obtained from the measured LAI and radiation attenuation through the canopy, which was calculated from solar radiation above and below the canopy. Assuming the extinction coefficient to be constant, daily LAI was estimated from the attenuation of solar radiation between 09:00 and 15:00 (Watanabe et al., 2001).

3. Results and discussions

3.1. Meteorological conditions and phenology

Snow accumulated over the forest floor from the beginning of December to the begining of April. The snow depth reached about 1 m at the end of February. The larch began to change its leaf color to yellow at the beginning of October, and the leaves fell by the middle of November. In the beginning of May, the new leaves emerged and began to develop.

Seasonal variations in air and soil temperatures, precipitation, incident PPFD, daytime VPD, LAI, albedo and NDVI are shown in Fig. 2, from September 2000 to August 2001; the data are integrated every 10 d, respectively. Daily mean air temperature at a height of 14 m ranged from –12 °C in January and February to 21 °C in July and August, and annual mean was 6.0 °C. Daily mean soil temperature at a depth of 5 cm ranged from –0.1 °C immediately after thaw in the middle of April to 20 °C in August, and the annual mean was 7.4 °C. Under the snow cover the temperature was almost constant between 0.1 and 0.2 °C. There was no clear seasonal variation in precipitation. The annual sum was 1265 mm and the sum for the leaf season from May to October was 962 mm. Incident PPFD was highest in April and May, and dropped significantly in July because of advection fog coming from the Pacific Ocean. The annual sum of PPFD was 7.5 kmol m^{-2} and the sum for the leaf season was 4.4 kmol m^{-2}. Daytime VPD at 14 m was relatively high in spring

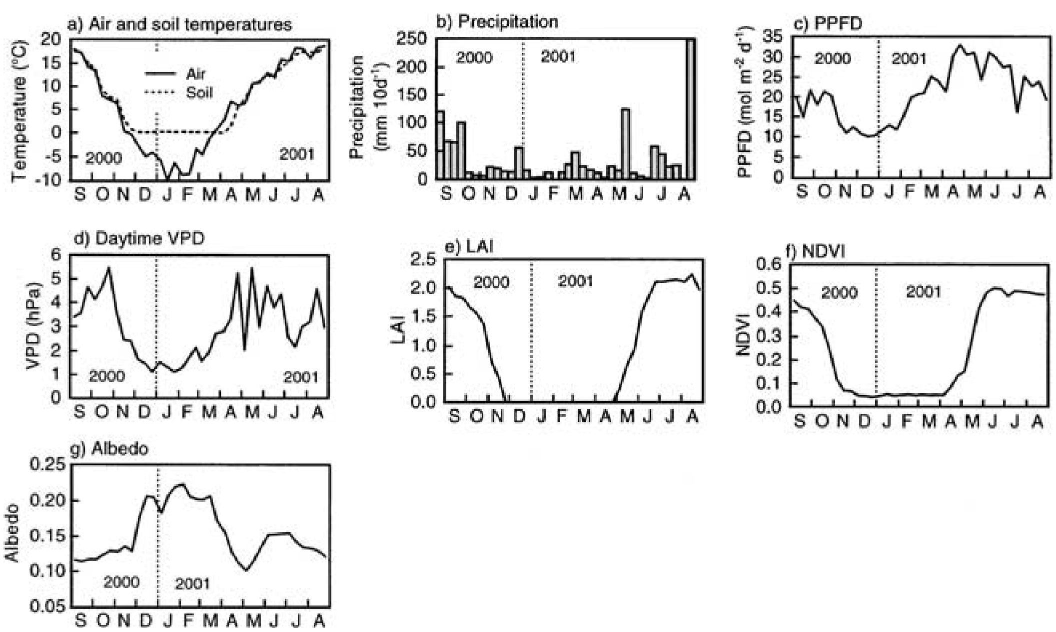

Fig. 2. Seasonal variations in (a) air temperature at a height of 14 m and soil temperature at a depth of 5 cm, (b) precipitation, (c) photosynthetic photon flux density (PPFD), (d) daytime (09:00–15:00 in JST) average vapor pressure deficit (VPD) at 14 m, (e) leaf area index (LAI) of the canopy, (f) NDVI between 09:00 and 15:00 and (g) albedo. Values integrated over 10 d are shown. The forest floor was covered with snow from the beginning of December to that of April.

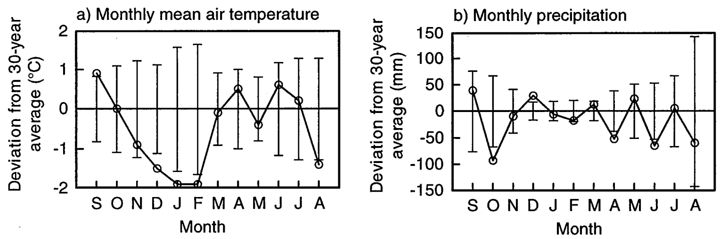

Fig. 3. Seasonal variation in deviation from the 30-yr average between 1971 and 2000 in monthly mean air temperature and monthly integrated precipitation, between September 2000 and August 2001 at Tomakomai Meteorological Station. Vertical bars denote the standard deviation of the 30-yr data.

and fall, yet never reached 6 hPa. LAI of the canopy rapidly increased in May and reached a plateau at 2.1 m^2 m^{-2} in the middle of June. It began to decrease in September and reached zero at the beginning of November. Since LAI of fern on the forest floor was about 3 m^2 m^{-2} in late June 2001, LAI of the forest reached at least 5 m^2 m^{-2} in summer. NDVI increased immediately after thaw, and the increase accelerated in May along with the increase in the canopy LAI. It reached a plateau at 0.5 in the middle of June and began to decrease in September. Albedo was 0.20–0.22 when there was snow cover and no leaves, and lower during the leaf season.

The climate of the year was compared with the average for 30 yr between 1971 and 2000, using the data measured at Tomakomai Meteorological Station (42°37′N, 141°33′E, 6 m above sea level), which is 14 km from the larch forest. Figure 3 shows the seasonal variation of the deviation from the 30-yr average in monthly values of air temperature and precipitation. Air temperature was low beyond the standard deviation (SD) of the 30-yr data in winter, December to February. Precipitation was small beyond the SD in April, June and October, while it was larger in December. Annual mean temperature and total precipitation were 7.0 °C and 1030 mm as compared to 7.5 ± 0.6 °C and 1226 ± 162 mm for the 30-yr average. Mean temperature and total precipitation during the leaf season, May–October, were 14.8 °C and 731 mm as compared to 14.8±0.7 °C and 883±203 mm for the 30-yr average; the precipitation was 83% of the 30-yr average.

3.2. *Energy balance closure*

Energy balance was not closed at this site as reported from other forests (e.g. Goulden et al., 1996; Aubinet et al., 2000; Wilson et al., 2002). The relationship between the half-hourly eddy flux of energy [the sum of sensible heat flux (H) and latent heat flux (lE)] and the available energy ($R_n - G$) is shown in Fig. 4, where R_n is net radiation and G soil heat flux. The slope of the linear regression for the snowless and snow seasons was 0.75 and 0.57, respectively. This value is used to

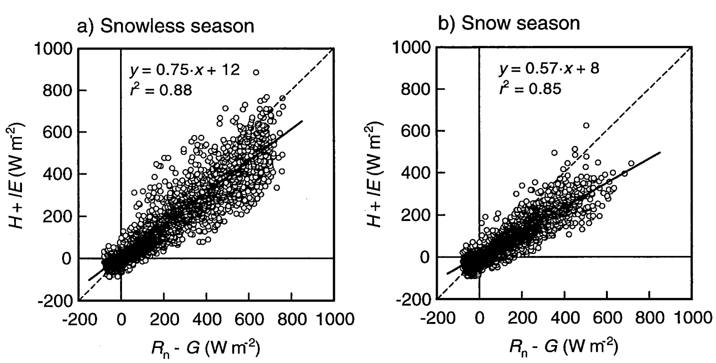

Fig. 4. Relationships between half-hourly eddy flux of energy ($H + lE$) against available energy ($R_n - G$) during the snowless (11 April to 30 November) and snow (1 December to 10 April) seasons.

evaluate energy balance closure (Aubinet et al., 2000; Wilson et al., 2002). The slope also differed with wind direction in the snowless season. Hereafter we divide all winds into two groups by direction, the south and north. The south and north winds are defined as the wind blowing from the south or north semicircle of the south side of the tower top on which the flux sensors were installed. Winds with direction between 73 and 253° are divided into the south wind considering the layout of the tower, and the others are the north wind. Thus the north wind comes to the flux sensors over or through the tower. In the snowless season, the slope and intercept were 0.77 and 9 W m^{-2} (r^2 = 0.89) for south wind and 0.63 and 13 W m^{-2} (r^2 = 0.89) for north wind. In the snow season, however, the slopes were very similar, 0.59 for the south and 0.57 for the north. The relative frequency of the south and north winds was 0.69 : 0.31 in the snowless season and 0.43: 0.57 in the snow season. The slope of 0.75 obtained in the snowless season is identical with that of one forest site (=0.756) in EUROFLUX obtained at temperatures higher than 1 °C (Aubinet et al., 2000). Wilson et al. (2002) evaluated the energy balance closure of 50 site-years in FLUXNET, and reported that the slope of $H + lE$ against $R_n - G - S$ ranged from 0.53 to 0.99 with a mean of 0.79, where S is the rate of change of heat storage. They also reported that the slope at forest sites increased by 7% on average by adding S. If this holds at our site, while S was not measured, the slope can be increased up to 0.80 for the snowless season. The overall energy balance ratio (EBR), the ratio of the total sums of $H + lE$ and $R_n - G$, was 0.82 over the year, and on a monthly basis EBR was larger than 0.9 between September and January and smaller than 0.7 in March and April. EBR for the snowless and snow seasons was 0.82 and 0.81, respectively; the closure was seemingly improved by comparison with the half-hourly evaluation (Fig. 4) because the underestimate and overestimate of eddy flux measurements cancelled each other (Mahrt, 1998; Wilson et al, 2002). The annual EBR of 0.82 is within the range at the FLUXNET sites, with a mean of 0.84 (Wilson et al., 2002).

The distribution of the friction velocity (u^*) is shown in Fig. 5 for the south and north winds. u^* was higher for the south wind than for the north wind in the snowless season, while the u^* distribution did not vary with wind direction in the snow season. Energy balance was more closed at higher u^* values, as noted in recent studies (Aubinet et al., 2000; Turnipseed et al., 2002; Wilson et al., 2002) (Fig. 6). The difference in the u^* distribution partly explains the difference in energy balance closure on a half-hourly basis (the slope in Fig. 6) between the south and north winds in the snowless season. In the snow season, however, although u^* was higher than in the snowless season, the slope was nevertheless smaller. This is inconsistent with a result measured at a subalpine forest in a snowy winter by Turnipseed et al. (2002). Their result showed that half-hourly energy balance closure was slightly better in the winter than in the summer, and it was mainly explained by higher u^* in the winter. We have no clear

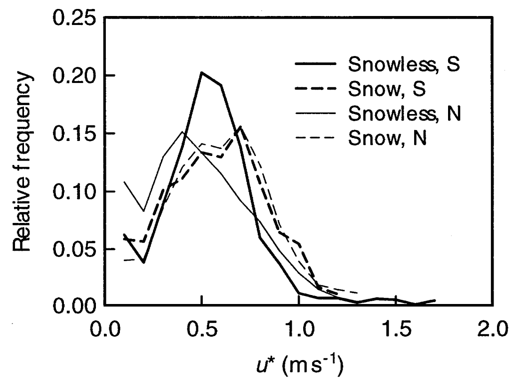

Fig. 5. Distribution of friction velocity (u^*) for the south and north winds during the snowless and snow seasons. Half-hourly data were binned by u^* into classes of 0.1 m s^{-1}.

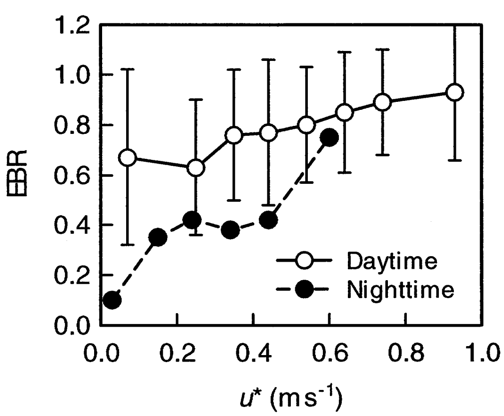

Fig. 6. Energy balance ratio [EBR = $(H + lE)/(R_n - G)$] plotted against u^* for daytime (10:00–15:00) and night-time, (19:00–05:00) under the condition of the south wind during the snowless season. Half-hourly data were binned by u^* into classes of 0.1 m s^{-1}. Vertical bars on the daytime plots denote SD; SD is omitted for the night-time plots because it is larger than one.

explanation for the lower closure in the snow season on a half-hourly basis. However, latent heat consumed by thaw in daytime or emitted by freeze at night probably left the energy balance open. Assuming that all of the precipitation was snow between December and March, the latent heat consumed by thaw was simply calculated at 76 MJ m^{-2}. Thus EBC for the snow season improved up to 1.0 by adding the latent heat of fusion.

Since the measuring height of 42 m is much higher than the canopy height of 15 m, part of the energy imbalance may be explained by insufficient fetch and advective flows (Lee, 1998; Finnigan, 1999; Yi et al., 2000). Moreover, inadequate detrending and large eddy fluctuations (Sakai et al., 2001) seem to be causes of the imbalance. Sakai et al. (2001) reported that detrending with a 30 min running mean and averaging for 3 h improved the energy balance closure of a deciduous temperate forest and a boreal forest for midday periods. However, their method cannot be applied to our data because the data were discontinuous; there were gaps for 2 min in the data every 30 min. Although there is a method to force the energy balance to close by partitioning available energy into H and lE using the Bowen ratio obtained from the eddy flux measurements (Twine et al., 2000), we did not apply the method to the data. Thus, such underestimates in the eddy fluxes of H and lE probably occurred in CO_2 flux, too.

3.3. *Dependence of NEE on environmental factors*

The relationship between half-hourly mean NEE and incident PPFD is shown in Fig. 7 for each month of the leaf season, from May to October. An empirical model based on Michaelis–Menten kinetics was used (Ruimy et al., 1995). Characteristic parameters obtained by curve fitting are listed in Table 1. The parameters include the ecosystem quantum yield efficiency (α, the initial slope of the curve), saturated NEE (NEE_s, the asymptotic value of NEE at infinite PPFD) and dark respiration rate (R_d, the value of NEE at PPFD

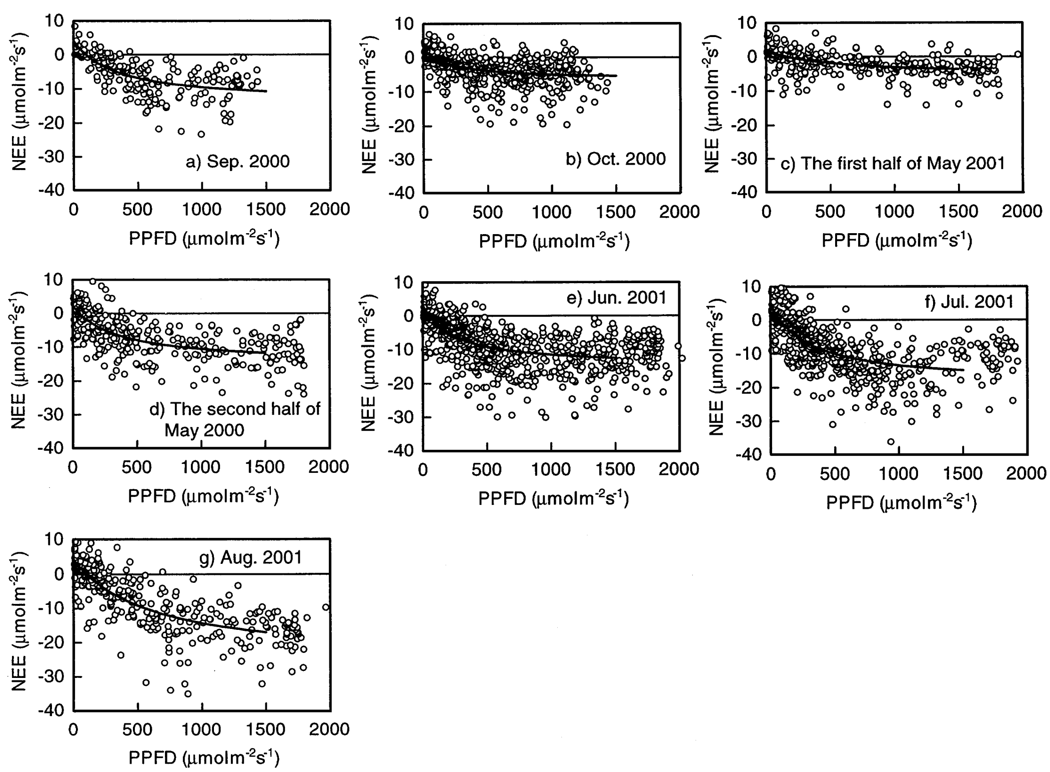

Fig. 7. Relationship between half-hourly NEE and incident PPFD in each month of the leaf season. A rectangular hyperbola was fitted to the relationship.

Table 1. *Parameters of the relationship between NEE and PPFD from a Michaelis–Menten model*

	α[a] (mol mol^{-1})	NEE$_s$[b] (μmol m^{-2} s^{-1})	R_d[c] (μmol m^{-2} s^{-1})	r^2
Sep. 2000	0.056	−18.1	4.2	0.48
Oct. 2000	0.044	−9.2	2.6	0.24
May 2001 (the first half)	0.015	−7.3	1.8	0.25
May 2001 (the second half)	0.051	−17.3	2.3	0.43
Jun. 2001	0.078	−18.3	3.3	0.40
Jul. 2001	0.079	−23.5	4.7	0.50
Aug. 2001	0.061	−30.3	4.4	0.61

[a]Ecosystem quantum yield efficiency.
[b]Saturated NEE.
[c]Dark respiration rate.

of zero). α changed seasonally; it increased from 0.015 mol (CO_2) mol^{-1} (photons) in the first half of May to 0.079 mol mol^{-1} in July, and decreased to 0.044 mol mol^{-1} in October. The seasonal change was similar to LAI (Fig. 2). The value of α obtained in summer is larger than those of other temperate forests; 0.029–0.044 mol mol^{-1} at an evergreen conifer forest (Aubinet et al., 2001), 0.021–0.063 mol mol^{-1} at a deciduous forest (Pilegaard et al., 2001), 0.044 mol mol^{-1} at a slash pine plantation (Clark et al., 1999), 0.04–0.06 mol mol^{-1} at Harvard Forest (Wofsy et al., 1993) and 0.037 and 0.024 mol mol^{-1} for the mean value of large number of broadleaf and conifer forests, respectively (Ruimy et al., 1995). NEE$_s$ decreased from −7.3 μmol m^{-2} s^{-1} in the first half of May to −30.3 μmol m^{-2} s^{-1} in August, and increased to −9.2 μmol m^{-2} s^{-1} in October. The NEE$_s$ value is compatible with those of other forests, such as an evergreen conifer forest in Europe (Aubinet et al., 2001). However, it is considerably more negative than that of a larch (*Larix gmelinii*) forest in eastern Siberia, which was −5 μmol m^{-2} s^{-1} in July (Hollinger et al., 1998). This small CO_2 uptake in Siberia was mainly caused by dryness and nitrogen deficiency. Since it was moist and VPD was low at our site, even in summer no drought effect was found. R_d also changed seasonally; it increased from 1.8 μmol m^{-2} s^{-1} in the first half of May to 4.7 μmol m^{-2} s^{-1} in July, and decreased to 2.6 μmol m^{-2} s^{-1} in October. The model using the parameters in Table 1 was applied to fill gaps in daytime NEE in the leaf season.

To calculate ecosystem respiration (RE) and fill gaps in night-time NEE, exponential equations were fitted to NEE and air temperature at 14 m for night-time in the leaf season and for the whole day in the leafless season, November–April (Fig. 8). During the leaf season night-time NEE evaluated at air temperatures of 0 and 20 °C was 0.8 and 4.2 μmol m^{-2} s^{-1} with a u^* threshold of 0.0 m s^{-1}, and 1.4 and 4.7 μmol m^{-2} s^{-1} with that of 0.2 m s^{-1}, respectively. These rates are within the range of those of other forests (Clark et al., 1999).

NEE was also compared between the south and north winds in five PPFD categories using the data obtained in June–August 2000 (Fig. 9). Although PPFD, air temperature and u^* were almost identical between the two wind directions in each PPFD category, NEE for the south wind was significantly more negative than for the north wind for PPFD higher than 10 μmol m^{-2}

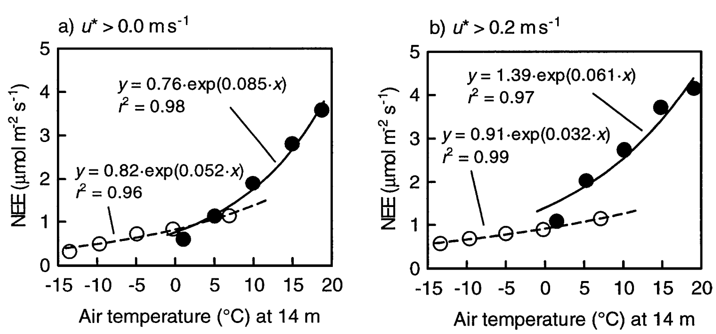

Fig. 8. Relationship between half-hourly NEE and air temperature at a height of 14 m for night-time in the leaf season (filled circles) and whole day in the leafless season (open circles) with a u^* threshold of 0.0 or 0.2 m s^{-1} at 42 m. The leaf season is May–October and the leafless season is November–April. Each circle is the mean for half-hourly NEE binned into 5 °C classes. An exponential curve was fitted to each relationship.

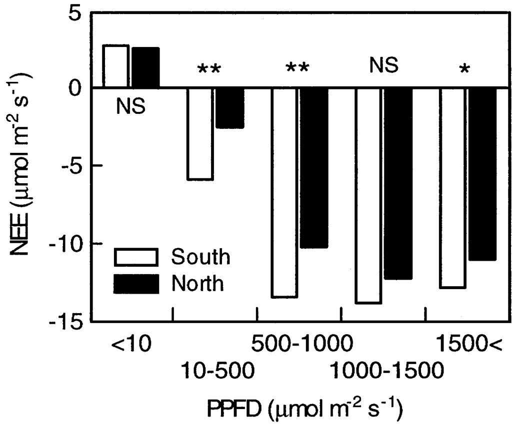

Fig. 9. Comparisons of mean NEE between the south and north wind conditions. Half-hourly NEE in June, July and August 2001 was binned into five PPFD categories. * and ** denote significant differences by the *t*-test in NEE between the two wind directions at $p < 0.05$ and $p < 0.01$, respectively. NS denotes no significant difference.

s^{-1}. Wilson et al. (2002) showed that daytime CO_2 flux was less negative under the condition of lower energy balance closure. The significant difference in daytime NEE with wind direction was probably caused by the difference in footprint and energy balance closure, and flow distortion by the tower.

3.4. Seasonal variations in NEE, evapotranspiration and energy fluxes

Seasonal variations in daily sums of NEE, RE, gross primary production (GPP), net radiation (R_n), sensible heat flux (H), latent heat flux (lE) and daytime-average Bowen ratio are shown in Fig. 10, from September 2000 to August 2001; GPP was calculated by subtracting RE from NEE. The monthly values of these series are also shown in Table 2, together with soil heat flux (G), evapotranspiration (E), precipitation (P) and air temperature (T_a). In addition, cumulative NEE, RE, GPP and E for the year are given in Fig. 11. In the figures and table all flux data were used regardless of wind direction, and gaps in RE were filled with a u^* thereshold of 0.2 m s^{-1} (Fig. 8).

GPP gradually approached zero in September and October as the senescence, the yellow coloring and fall of the larch leaves progressed, and it began to become more negative in the middle of April, immediately after thaw. In May, GPP rapidly decreased as the larch leaves developed (Fig. 2), and it was stable between -0.55 and -0.65 mol m^{-2} d^{-1} from the beginning of June to the middle of August. GPP in late April was due to the photosynthesis of vegetation on the forest floor. Since the fern is an evergreen, it photosynthesizes before the leaf emergence of the trees. Moreover, the understory grasses leaf out in advance of the trees. On the other hand, RE changed with the seasonal variation in temperature; it decreased from September to November and increased from April to August. As a result, NEE was negative for the leaf season, from May to October with a peak intensity of -0.38 mol m^{-2} d^{-1}at the middle of June. A positive NEE in September (Fig. 9) was probably caused by light deficiency due to the large amount of precipitation (Fig. 2). NEE during the leafless and snow seasons ranged between 0 and 0.05 mol m^{-2} d^{-1}.

H was small during the fall (Fig. 9). H gradually increased from January and rapidly increased in the middle of April. In May and June H gradually decreased with the leaf expansion of the trees, while lE increased. Consequently, the daytime Bowen ratio decreased in May and June, and it was less than one in July–September.

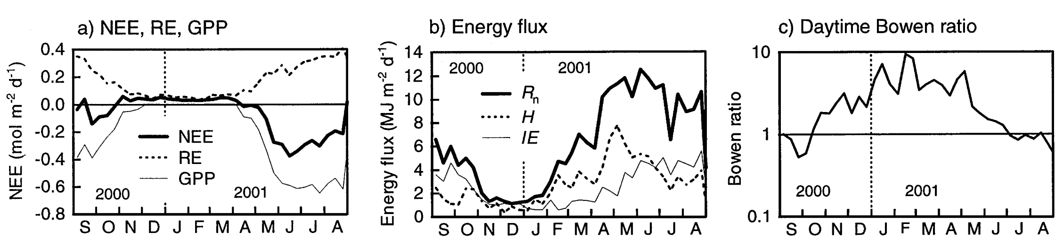

Fig. 10. Seasonal variations in (a) NEE, RE and GPP, (b) net radiation (R_n), sensible heat flux (H) and latent heat flux (lE) and (c) daytime (09:00–15:00 in JST) average Bowen ratio (H/lE). Values integrated over 10 d are shown. All flux data were used regardless of wind direction, and gaps in RE were filled with a u^* threshold of 0.2 m s^{-1}.

Table 2. *Monthly values of NEE, gross primary production (GPP), ecosystem respiration (RE), net radiation (R_n), sensible heat flux (H), latent heat flux (lE), soil heat flux (G), evapotranspiration (E), precipitation (P) and air temperature at a height of 14 m (T_a)*

	NE E (mol m^{-2})	RE (mol m^{-2})	GPP (mol m^{-2})	R_n (MJ m^{-2})	H (MJ m^{-2})	lE (MJ m^{-2})	G (MJ m^{-2})	E (mm)	P (mm)	T_a (°C, 14 m)
Sep. 2000	−1.4	9.3	−10.7	173	51	112	−4	45	251	16.4
Oct. 2000	−1.8	5.6	−7.4	140	61	93	−12	37	119	9.4
Nov. 2000	1.4	2.6	−1.2	47	30	35	−14	14	49	2.1
Dec. 2000	1.4	1.9	−0.5	33	17	33	−10	13	83	−4.0
Jan. 2001	1.8	1.8	0.0	55	39	21	−7	8	23	−7.3
Feb. 2001	1.3	1.3	0.0	115	75	25	−5	10	25	−7.2
Mar. 2001	2.1	2.1	0.0	194	99	41	−4	16	97	−1.7
Apr. 2001	−0.3	2.7	−3.0	292	151	59	5	23	33	5.1
May. 2001	−4.6	6.9	−11.5	339	186	99	11	39	163	9.3
Jun. 2001	−10.5	7.9	−18.4	362	147	136	8	54	20	13.7
Jul. 2001	−8.4	10.0	−18.4	260	80	130	9	52	126	17.3
Aug. 2001	−5.4	11.4	−16.8	280	92	140	5	56	275	17.8
Annual	−24.4	63.5	−87.9	2290	1028	924	−18	367	1265	5.9

Annual sums of NEE, RE and GPP were evaluated by four methods (Table 3). These were the combinations of two data sets and two exponential models; the data sets included (1) all wind or (2) only the south wind, and the exponential equations were derived with a u^* thereshold of (a) 0.0 m s^{-1} or (b) 0.2 m s^{-1}. In Figs. 10 and 11 and Table 2, the combination of (1) and (a) was applied. Annual NEE, RE and GPP were −24.4 to −32.4 (=−293 to −389), 54.9 to 65.5 (= 659 to 786) and −84.3 to −94.9 mol m^{-2} yr^{-1} (= −1012 to −1139 gC m^{-2} yr^{-1}), respectively. The ranges of the evaluations were 8.0, 10.7 and 10.6 mol m^{-2} yr^{-1} for NEE, RE and GPP, respectively.

Annual NEE at the larch forest is within the range of those measured at temperate forests in North America and West Europe (Baldocchi et al., 2001), while it is less negative than that of EUROFLUX sites compared at the same latitude (Valentini et al., 2000). Moreover, annual RE is smaller and annual GPP is less negative at our site than the averages obtained at the EUROFLUX sites, which are 1100 and –1380 gC m^{-2} yr^{-1} for RE and GPP, respectively (Jansens et al., 2001). However, NEE at the larch forest is about 1.5 times as negative as −219 and −256 gC m^{-2} yr^{-1} measured in 2000 at a neighboring broadleaf deciduous forest (Tanaka et al., 2001) and a broadleaf deciduous forest (Nakai et al., 2003) 30 km from the larch forest, respectively. The latter forest had RE and GPP of 857 and −1113 gC m^{-2} yr^{-1}, respectively. The stem production of larch plantations growing in relatively favorable environments ranged from 4.1 to 6.7 t (dry matter) ha^{-1} yr^{-1} (Gower and Richards, 1990). If the dry matter is only composed of cellulose, the production rate corresponds to 1.8–2.9 tC ha^{-1} yr^{-1}. The difference between NEE of −2.9 to −3.9 tC ha^{-2} yr^{-1} at our site and the production rate is partly explained by the production of

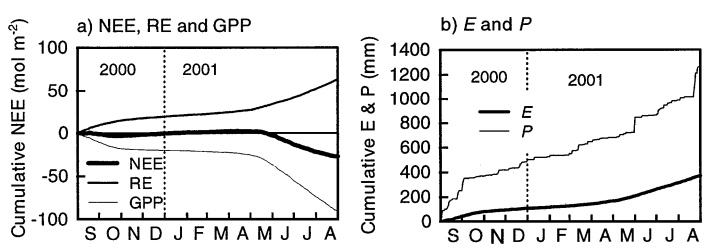

Fig. 11. Cumulative (a) NEE, RE and GPP and (b) evapotranspiration (*E*) and precipitation (*P*) for the year, from September 2000 to August 2001.

Table 3. *Comparison of annual NEE, RE and GPP evaluated by four methods*

	Method[a]	NEE (mol m^{-2} yr^{-1})	RE (mol m^{-2} yr^{-1})	GPP (mol m^{-2} yr^{-1})
Annual total	(1) + (a)	−29.4	54.9	−84.3
	(1) + (b)	−24.4	63.5	−87.9
	(2) + (a)	−32.4	57.0	−89.4
	(2) + (b)	−29.4	65.5	−94.9

[a]Half-hourly flux data were used for (1) all wind or (2) only the south wind, and exponential equations (Fig. 8) were derived with a u^* threshold of (a) 0.0 or (b) 0.2 m s^{-1}.

understory vegetation, and roots and leaves of the larch in the forest. Baldocchi et al. (2001) showed a simple relationship between annual NEE and the length of growing season defined as the periods over which mean daily NEE was negative, using the FLUXNET data. The growing season was 174 d at the larch forest for the year. The estimated annual NEE of −394 gC m^{-2} yr^{-1} from the relationship is compatible with the measured NEE.

The annual sum of E was 367 mm (Table 2); this was 29% of the annual P(=1265 mm), and the corresponding lE was 40% of the annual R_n (= 2368 MJ m^{-2}) (Fig. 11). The annual E at the larch forest is smaller than that of 400–430 mm at a ponderosa pine forest with the same value of P in Oregon, USA (Anthoni et al., 1999) and a two-year accumulated E of 1331 mm at a maritime pine forest in France with accumulated P of 1860 mm (Berbigier et al., 2001). Low VPD during the growing season at the larch forest caused a decrease in evapotranspiration. At the larch forest, much of precipitation infiltrated into the volcanic soil with high permeability. In addition, EBC was 85% on an annual basis, and it increased to 88% by adding the latent heat of thaw.

4. Conclusions

Eddy fluxes of CO_2 and water vapor have been measured since 2000 over a deciduous conifer forest (a larch plantation) in northern Japan. The fluxes changed seasonally in accordance with the annual cycles of the larch phenology and climate. Annual NEE from September 2000 to August 2001 was −24.4 to −32.4 mol m^{-2} yr^{-1} (= −293 to −389 gC m^{-2} yr^{-1}); this value is compatible with those reported from other temperate forests. Annual evapotranspiration for the same period was 367 mm, which was only 29% of annual precipitation. However, there is a remaining uncertainty in the flux measurements, because the energy balance is not closed.

5. Acknowledgements

We acknowledge the Hokkaido Regional Office of the Forestry Agency for use of the larch plantation, Keiji Okada for the footprint calculation, Takayoshi Koike for useful comments on the LAI measurements, Yasuyuki Kitamori and Tetsuhiro Yorisaki for the maintenance of the instruments, Atsushi Toriyama for the management of the meteorological data, Kazuhiro Sugimoto for the measurements and calculations of LAI, Hiroshi Matsuura for modifying the programs to calculate fluxes, and Takeo Yuzu and Rei Fujita for supplying data on the stand density. We are grateful to two anonymous referees for very helpful comments and suggestions.

REFERENCES

Anthoni, P. M., Law, B. E. and Unsworth, M. H. 1999. Carbon and water vapor exchange of an open-canopied ponderosa pine ecosystem. *Agric. For. Meteorol* **95**, 151–168.

Aubinet, M., Grelle, A., Ibrom, A., Rannik, Ü., Moncrieff, J., Foken, T., Kowalski, A. S., Martin. P. H., Berbigier, P., Bernhofer, Ch., Clement, R., Elbers, J., Granier, A., Grunwald, T., Morgenstern, K., Pilegaard, K., Rebmann, C., Snijders, W., Valentini, R., Vesala, T. 2000. Estimates of the annual net carbon and water vapor exchange of forests: the EUROFLUX methodology. *Adv. Ecol. Res.* **30**, 113–175.

Aubinet, M., Chermanne, B., Vandenhaute, M., Longdoz, B., Yernaux, M. and Laitat, E. 2001. Long term carbon dioxide exchange above a mixed forest in the Belgian Ardennes. *Agric. For. Meteorol.* **108**, 293–315.

Auble, D. and Meyers, T. P. 1992. An open path, first response infrared absorption gas analyzer for H_2O and CO_2. *Bound.-Layer Meteorol.* **59**, 243–256.

Baldocchi, D., Falge, E., Gu, L., Olson, R., Hollinger, D., Running, S., Anthoni, P., Bernhofer, C., Davis, K., Evans, R., Fuentes, J., Goldstein, A., Katul, G., Law, B., Lee, X., Malhi, Y., Meyers, T., Munger, W., Oechel, W., Paw, U. K. T., Pilegaard, K., Schmid, H. P., Valentini, R., Verma, S., Vesala, T., Wilson, K. and Wofsy, S. 2001. FLUXNET: A new tool to study the temporal and spatial variability of ecosystem-scale carbon dioxide, water vapor, and energy flux densities. *Bull. Am. Meteorol. Soc*. **82**, 2415–2434.

Berbigier, P., Bonnefond, J. and Mellmann, P. 2001. CO_2 and water vapor fluxes for 2 years above Euroflux forest site. *Agric. For. Meteorol*. **108**, 183–197.

Clark, K. L., Gholz, H. L., Moncrieff, J. B., Cropley, F. and Loescher, H. W. 1999. Environmental controls over net exchange of carbon dioxide from contrasting Florida ecosystems. *Ecol. Appl*. **9**, 936–948.

Denning, A. S., Fung, I. Y. and Randall, D. 1995. Latitudinal gradient of atmospheric CO_2 due to seasonal exchange with land and biota. *Nature* **376**, 240–243.

Falge, E., Baldocchi, D., Olson, R., Anthoni, P., Aubinet, M., Bernhofer, C., Burba, G., Ceulemans, R., Clement, R., Dolman, H., Granier, A., Gross, P., Grünwald, T., Hollinger, D., Jensen, N., Katul, G., Keronen, P., Kowalski, A., Lai, C. T., Law, B. E., Meyers, T., Moncrieff, J., Moors, E., Munger, W., Pielegaard, K., Rannik, Ü., Rebmann, C., Suyker, A., Tenhunen, J., Tu, K., Verma, S., Vesala, T., Wilson, K. and Wofsy, S. 2001a. Gap filling strategies for defensible annual sums of net ecosystem exchange. *Agric. For. Meteorol*. **107**, 43–69.

Falge, E., Baldocchi, D., Olson, R., Anthoni, P., Aubinet, M., Bernhofer, C., Burba, G., Ceulemans, R., Clement, R., Dolman, H., Granier, A., Gross, P., Grünwald, T., Hollinger, D., Jensen, N., Katul, G., Keronen, P., Kowalski, A., Lai, C. T., Law, B. E., Meyers, T., Moncrieff, J., Moors, E., Munger, W., Pielegaard, K., Rannik, Ü., Rebmann, C., Suyker, A., Tenhunen, J., Tu, K., Verma, S., Vesala, T., Wilson, K. and Wofsy, S. 2001b. Gap filling strategies for long term energy flux data sets. *Agric. For. Meteorol*. **107**, 71–77.

Finnigan, J. 1999. A comment on the paper by Lee (1998): "On micrometeorological observations of surface–air exchange over tall vegetation." *Agric. For. Meteorol*. **97**, 55–64.

Fujinuma, Y., Takada, M., Tashiro, K. and Inoue, G. 2001. GHGs flux monitoring at larch forest in Hokkaido, Japan. *CGER-Report* **M-011** (Proc. International Workshop for Advanced Flux Network and Flux Evaluation), 161–164.

Goulden, M. L., Munger, J. W., Fan, S. M., Daube, B. C. and Wofsy, S. C. 1996. Measurements of carbon sequestration by long term eddy co-variance: methods and a critical evaluation of accuracy. *Global Change Biol*. **2**, 169–182.

Gower, S. T. and Richards, J. H. 1990. Larches: deciduous conifers in an evergreen world. *BioScience* **40**, 818–826.

Greco, S. and Baldocchi, D. 1996. Seasonal variations of CO_2 and water vapor exchange rates over a temperate deciduous forest. *Global Change Biol*. **2**, 183–197.

Hignett, P. 1992. Corrections to temperature measurements with a sonic anemometer. *Bound.-Layer Meteorol*. **61**, 175–187.

Houghton, R. A., Davidson, E. A. and Woodwell, G. M. 1998. Missing sinks, feedbacks, and understanding the roll of terrestrial ecosystems in the global carbon balance. *Global Biogeochem. Cycles* **12**, 25–34.

Hollinger, D. Y., Kelliher, F. M., Schulze, E. D., Bauer, G., Arneth, A., Byers, J. N., Hunt, J. E., McSeveny, T. M., Kobak, K. I., Milukova, I., Sogatchev, A., Tatarinov, F., Varlargin, A., Ziegler, W. and Vygodskaya, N. 1998. Forest–atmosphere carbon dioxide exchange in eastern Siberia. *Agric. For. Meteorol*. **90**, 291–306.

Jansens, I. A., Lankreijer, H., Matteccui, G., Kowalski, A. S., Buchmann, N., Epron, D., Pilegaard, K., Kutsch, W., Longdoz, B., Grünwald, T., Montagnani, L., Dore, S., Rebmann, C., Moors, E. J., Grelle, A., Rannik, Ü., Morgenstern, K., Oltchev, S., Clement, R., Gudmundsson, J., Minerbi, S., Berbigier, P., Ibron, A., Moncrieff, J., Aubinet, M., Bernhofer, C., Jensen, N. O., Vesala, T., Granier, A., Schulze, E.-D., Lindroth, A., Dolman, A. J., Jarvis, P. G., Ceulemans, R. and Valentini, R. 2001. Productivity overshadows temperature in determining soil and ecosystem respiration across European forests. *Global Change Biol*. **7**, 269–278.

Kaimal, J. C. and Gaynor, J. E. 1991. Another look at sonic thermometry. *Bound.-Layer Meteorol*. **56**, 401–410.

Kormann, R. and Mexiner, F. X. 2001. An analytical footprint model for non-neutral stratification. *Bound.-Layer Meteorol*. **99**, 207–224.

Lee, X. 1998. On micrometeorological observations of surface-air exchange over tall vegetation. *Agric. For. Meteorol*. **91**, 39–49.

Machimura, T. and Fukuda, M. 2001. Operation of flux stations in east Siberian Taiga forest. *CGER-Report* **M-011** (Proc. International Workshop for Advanced Flux Network and Flux Evaluation), 83–86.

Mahrt, L. 1998. Flux sampling errors for aircraft and towers. *J. Atom. Ocean. Technol*. **15**, 416–429.

McMillen, R. T. 1988. An eddy correlation technique with extended applicability to non-simple terrain. *Bound.-Layer Meteorol*. **43**, 231–245.

Nakai, Y., Kitamura, K., Suzuki, S. and Abe, S. 2003. Yearlong carbon dioxide exchange above a broadleaf deciduous forest in Sapporo, northern Japan. *Tellus* **55B**, this issue.

Nakai, Y., Saigusa, N., Hirano, T., Evans, R., Ohtani, Y., Hirata, R., Toriyama, A., Kitamura, K., Suzuki, S., Yamamoto, S. 2002. A field experiment in August 2002 for the comparison of eddy-flux systems between AsiaFlux and AmeriFlux. *J. Jpn. Soc. Hydrol Water Resour*. **15**, 665–672. (in Japanese)

Otto-Bliesner, B. L. and Upchurch, G. R., Jr. 1997. Vegetation-induced warming of high latitude regions during the late cretaceous period. *Nature* **385**, 804–807.

Pilegaard, K., Hummelsøj, P., Jenzen, N. O. and Chen, Z. 2001. Two year continuous CO_2 eddy-flux measurements over a Danish beech forest. *Agric. For. Meteorol*. **107**, 29–41.

Ruimy, A., Jarvis, P. G., Baldocchi, D. D. and Saugier, B. 1995. CO_2 fluxes over plant canopies and solar radiation. *Adv. Ecol. Res*. **26**, 1–69.

Sakai, R. K., Fitzjarrald, D. R. and Moore, K. E. 2001. Importance of low-frequency contributions to eddy fluxes observed over rough surfaces. *J. Appl. Meteorol*. **40**, 2178–2192.

Tanaka, Y., Tanaka, N. and Hatano, R. 2001. Seasonal variation of carbon dioxide and energy fluxes above a cool, temperate, broad-leaved forest. *CGER-Report* **M-011** (Proc.

International Workshop for Advanced Flux Network and Flux Evaluation), 133–137.
Turnipseed, A. A., Blanlen, P. D., Anderson, D. E. and Monson, R. K. 2002. Energy budget above a high-elevation subalpine forest in complex topography. *Agric. For. Meteorol*. **110**, 177–201.
Twine, T. E., Kustas, W. P., Norman, J. M., Cook, D. R., Houser P. R., Meyers, T. P., Prueger, J. H., Starks, P. J. and Wesley, M. L. 2000. Correcting eddy-covariance flux underestimates over a grassland. *Agric. For. Meteorol*. **103**, 279–300.
Valentini, R., Matteucci, G., Dolman, A. J., Schulze, E.-D., Rebmann, C., Moors, E. J., Granier, A., Gross, P., Jensen, N. O., Pilegaard, K., Lindroth, A., Grelle, A., Bernhofer, C., Grünwald, T., Aubinet, M., Ceulemans, R., Kowalski, A. S., Vesala, T., Rannik, Ü., Berbigier, P., Loustau, D., Guomundsson, J., Thorgirsson, H., Ibrom, A., Mogenstern, K., Clement, R., Moncrieff, J., Montagnani, L., Minebi, S. and Jarvis, O. G. 2000. Respiration as the main determinant of carbon balance in Europe forests. *Nature* **404**, 861–865.
Watanabe, T., Yasuda, Y., Yamanoi, K., Ohtani, Y., Okano, M. and Mizoguchi, Y. 2001. Seasonal variations in energy and CO_2 fluxes over a temperate deciduous forest at Kawagoe, Japan. *CGER-Report* **M-011** (Proc. International Workshop for Advanced Flux Network and Flux Evaluation), 11–17.
Webb, E. K., Pearman, G. I. and Leuning, R. 1980. Correction of flux measurements for density effects due to heat and water vapour transfer. *Q. J. R. Meteorol. Soc*. **106**, 85–100.
Wilson, K., Goldstein, A., Falge, E., Aubinet, M., Baldocchi, D., Berbigier, P., Bernhofer, C., Ceulemans, R., Dolman, H., Field, C., Grelle, A., Ibrom, A., Law, B., Kowalski, A., Meyers, T., Moncrieff, J., Monson, R., Oechel, W., Tenhunen, J., Valentini, R. and Verma, S. 2002. Energy balance closure at FLUXNET sites. *Agric. For. Meteorol*. **113**, 223–343.
Wofsy, S. C., Goulden, M. L., Munger, J. W., Fan, S. W., Bakwin, P. S., Daube, B. C., Bassow, S. L. and Bazzaz F. A. 1993. Net exchange of CO_2 in a mid-latitude forest. *Science* **260**, 1314–1317.
Yi, C., Davis, K. J., Bakwin, P. S., Berger B. W. and Marr, L. C. 2000. Influence of advection on measurements of the net ecosystem-atmosphere exchange of CO_2 from a very tall tower. *J. Geophys. Res*. **105**, 9991–9999.